IEEE Access
Multidisciplinary ⋮ Rapid Review ⋮ Open Access Journal

Received 22 July 2023, accepted 18 August 2023, date of publication 22 August 2023, date of current version 25 August 2023.

Digital Object Identifier 10.1109/ACCESS.2023.3307407

RESEARCH ARTICLE

Deep Learning-Based Resource Allocation Scheme for Heterogeneous NOMA Networks

DONGHYEON KIM[1], (Graduate Student Member, IEEE), SEAN KWON[2], (Member, IEEE), HAEJOON JUNG[1], (Senior Member, IEEE), AND IN-HO LEE[3], (Senior Member, IEEE)

[1]Department of Electronics and Information Convergence Engineering, Kyung Hee University, Yongin-si 17104, South Korea
[2]Department of Electrical Engineering, California State University Long Beach, Long Beach, CA 90840, USA
[3]School of Electronic and Electrical Engineering, Hankyong National University, Anseong-si 17579, South Korea

Corresponding authors: In-Ho Lee (ihlee@hknu.ac.kr) and Haejoon Jung (haejoonjung@khu.ac.kr)

This work was supported in part by the Korean Government, in part by the National Research Foundation of Korea under Grant NRF-2022R1A2C1003388 and Grant NRF-2022R1A4A3033401, in part by the ITRC Support Programs under Grant IITP-2023-2021-0-02046, and in part by the Convergence Security Core Talent Training Business Support Program Supervised by the IITP under Grant IITP-2023-RS-2023-00266615.

ABSTRACT In this paper, we consider downlink power-domain non-orthogonal multiple access (NOMA) in heterogeneous networks (HetNets) and propose resource allocation algorithms for subchannels and transmit powers to improve the sum rate performance while satisfying a minimum data-rate requirement. The proposed subchannel allocation scheme is an iterative algorithm to achieve NOMA gain by selecting the best subchannel from the viewpoint of each user, without the constraint of the number of NOMA users on each subchannel. The proposed power allocation scheme for NOMA is a deep neural network (DNN)-based unsupervised learning algorithm, where the output of the subchannel allocation scheme is used, and unsupervised learning is adopted to reduce the training complexity, as compared to supervised learning. Through simulation, we show that the proposed subchannel allocation scheme provides better sum rates compared to the conventional two-sided matching scheme, and the proposed power allocation scheme achieves a comparable sum rate to the interior point method (IPM).

INDEX TERMS Non-orthogonal multiple access, heterogeneous network, deep neural network, subchannel allocation, power allocation, sum rate.

I. INTRODUCTION

Non-orthogonal multiple access (NOMA) has been well-known as a promising technique to realize extremely high spectral efficiency for beyond 5G and 6G communications. In particular, the power-domain NOMA technique has attracted great attention in downlink cellular systems, where a base station (BS) superimposes and transmits data signals of multiple users, and then a user receives and decodes the signals with successive interference cancellation (SIC) [1]. Furthermore, the application of NOMA in heterogeneous networks (HetNets) has highlighted its capability that can meet the diverse requirements of users in future communications [2], [3]. However, it is challenging to improve the system performance (e.g., sum rate, spectral efficiency, and energy efficiency) in NOMA-enabled HetNet because of the large-scale interference between small cells.

For this reason, many resource allocation schemes such as user association, subchannel (i.e., frequency band) allocation, and transmit power allocation are proposed for interference management in the downlink NOMA-based HetNet [4], [5], [6]. In particular, the Lagrangian dual decomposition method is employed for user association in HetNets to relax the complexity of an objective function [7], [8]. In addition, the matching algorithm is adopted for subchannel allocation to improve the sum rate or energy efficiency by exploring the preferred subchannel [8], [9]. Moreover, various heuristic algorithms such as weighted minimum mean square error, fractional algorithm, and trust region interior point method (IPM) [10], [11], [12] are proposed for power allocation to maximize the sum rate, which is a crucial issue in the power-domain NOMA.

The associate editor coordinating the review of this manuscript and approving it for publication was Ayaz Ahmad.

The conventional resource allocation schemes are based on excessively iterative algorithms, which can incur high complexity. Therefore, in recent studies, the deep neural network (DNN)-based resource allocation methods are proposed to achieve lower complexity than the iterative algorithms. In [13], [14], and [15], the authors propose the DNN-based power allocation scheme with a supervised learning method. Supervised learning gets noticed in resource allocation because it can obviously guarantee a near-optimal performance. Although supervised learning is a magnificent method in resource allocation, if the time for generating labeled data increases, an unattainable complexity for training can occur because of a time-varying wireless environment. On the other hand, deep reinforcement learning-based algorithms are proposed to resolve the power allocation problems [12], [16], [17]. Although the reinforcement learning-based methods can avoid generating labeled data, they still require the training complexity of trial and error.

In contrast to the aforementioned training strategies, unsupervised learning-based resource allocation schemes are proposed to realize considerably less training complexity [18], [19], [20], [21]. Thus, in this paper, we focus on DNN-based resource allocation algorithms with the unsupervised training method to reduce the training complexity, which can be an alternative to compensate for the shortcomings of other machine learning algorithms. However, the conventional unsupervised manner cannot allow the binary nature of variables for the user association and subchannel allocation, which can be a critical problem in the HetNet and multi-carrier systems. Hence, for achieving flexible resource management in HetNet with multiple subchannels, we newly present the DNN structure and training method that can consider the user association and subchannel allocation indexes, which are the binary variables.

In [9], the power-domain NOMA is considered in a downlink single-cell system, and the two-stage resource allocation scheme is proposed to maximize the sum rate. In its first stage, the transmit powers for users in different subchannels are allocated by a DNN-based supervised learning algorithm, in which the results of the IPM are used as labeled data for training. In the second stage, based on the transmit powers allocated by the DNN-based supervised learning, the BS performs the iterative subchannel allocation scheme to choose the preferred matching subchannel for the users with high channel power. However, the supervised learning algorithm with IPM may require high complexity for training because the IPM is an iterative algorithm that becomes computationally expensive to solve large-scale problems.

In [8], the downlink HetNet using the power-domain NOMA is presented, and the user association, subchannel allocation, and power allocation schemes are proposed to maximize the energy efficiency. Especially, the user association scheme is based on the Lagrange dual decomposition method for load balancing and maximum energy efficiency. The subchannel allocation scheme uses the semi-supervised deep learning algorithm using the two-sided matching method to maximize the energy efficiency, where at most two users for NOMA can occupy a subchannel of each BS. However, this constraint of the number of users on a subchannel can limit an achievable NOMA gain. The transmit power allocation scheme is based on the DNN-based supervised learning algorithm, in which the labeled data to maximize energy efficiency is generated by an iterative gradient algorithm.

In this paper, we consider the downlink HetNet using the power-domain NOMA in the presence of the NOMA-user interference, the inner macro-cell interference, and the other macro-cell interference. Different from [8] and [9], we propose a subchannel allocation scheme with an iterative algorithm and a DNN-based power allocation scheme with unsupervised learning to maximize the sum rate and satisfy a minimum data-rate requirement. In the subchannel allocation scheme, a subchannel with the highest achievable data rate is selected for each user in the HetNet, which is not the same as conventional greedy scheduling[1], and more than two users can occupy a subchannel in order to enhance the NOMA gain in practice. Then, the power allocation scheme for NOMA uses the output of the subchannel allocation scheme. For power allocation for all NOMA users assigned to the subchannels, a DNN-based unsupervised learning algorithm is presented with a newly defined loss function without labeled data to reduce the training complexity. It is noted that the proposed unsupervised learning scheme can conduct transmit power allocation considering user association and subchannel allocation indicators, unlike the conventional unsupervised learning schemes in [18], [19], [20], and [21].

The major contributions of this paper are summarized as follows:

- The DNN-based resource allocation scheme using an unsupervised algorithm is proposed for the downlink NOMA-based HetNet with multiple subchannels to reduce its complexity, where we focus on user association, subchannel allocation, and power allocation to maximize the sum rate while achieving the minimum data-rate requirement.
- In particular, the subchannel allocation scheme using Lagrangian dual decomposition-based user association is proposed to obtain resource allocation indicators for maximizing the sum rate, and the DNN-based transmit power allocation scheme is also proposed based on the resource allocation indicators, which can allow more flexible transmit power allocation for NOMA.
- Through simulations, diverse performance comparisons are provided to show the effectiveness of the proposed scheme in terms of the sum rate, outage rate, and computational time, where the proposed scheme attains comparable or superior performance to the conventional

[1] In greedy scheduling, a user with the highest data rate is selected for each subchannel.

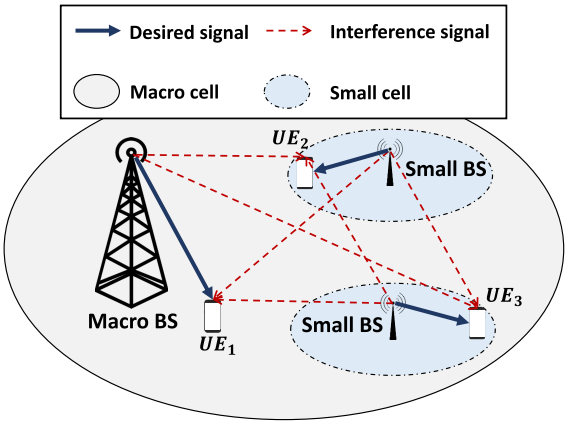

FIGURE 1. An example of downlink NOMA-based HetNet with one macro-BS, two small BSs, and three users.

two-sided matching and IPM-based schemes, despite its lower computational complexity.

II. SYSTEM MODEL

We consider a downlink NOMA-based HetNet with multiple small cells in a macro cell, as shown in Fig. 1, where all the BSs and users are equipped with a single antenna. Let $\mathcal{B} = \{1, 2, \cdots, b, \cdots, B\}$ denote the set of a macro BS and $B-1$ small BSs in the HetNet, $\mathcal{N} = \{1, 2, \cdots, n, \cdots, N\}$ denote the set of subchannels in the system bandwidth, and $\mathcal{M} = \{1, 2, \cdots, m, \cdots, M\}$ be the set of users in the HetNet.

We assume that each user is associated with one macro or small BS, and the set of user association indicators is denoted as $X = \{x_{1,1}, x_{1,2}, \cdots, x_{b,m}, \cdots, x_{B,M}\}$. If user m is associated with BS b, then, $x_{b,m} = 1$. Otherwise, $x_{b,m} = 0$. It is also assumed that each user uses one subchannel, and multiple users can be allocated to a subchannel for NOMA transmission. Then, the set of subchannel allocation indicators is denoted as $S = \{s^1_{1,1}, s^1_{1,2}, \cdots, s^n_{b,m}, \cdots, s^N_{B,M}\}$. If user m is allocated to subchannel n of BS b, then $s^n_{b,m} = 1$. Otherwise, $s^n_{b,m} = 0$.

The channel gain between BS b and user m on subchannel n is given as

$$h^n_{b,m} = |g^n_{b,m}|^2 d^{-\alpha}_{b,m}, \tag{1}$$

where $g^n_{b,m}$, $d_{b,m}$, and α are the Rayleigh-distributed random variable with zero mean and unit variance, the distance between BS b and user m, and the path-loss exponent, respectively. According to the NOMA protocol, a BS superimposes and transmits data signals of multiple associated users on a subchannel, and then each user receives the superposed signals and decodes its own desired signal by using SIC. At a user, the SIC operation is performed only for the stronger signals than its desired signal, and its order is from the strongest to the weakest signal [22]. In the downlink NOMA-based HetNet, the SIC decoding is based on the signal-to-interference-plus-noise-ratios (SINRs) rather than the channel gains [22].

In this paper, we assume that each user can obtain the received SINR by estimating the channel gains from the serving BS and the interfering BSs in a macro cell [23], and the macro BS can know all the channel gains perfectly. To determine the SIC order, the received SINR of user m for BS b on subchannel n is then obtained as [24]

$$\Gamma^n_{b,m} = \frac{s^n_{b,m} h^n_{b,m}}{I^n_{b,m} + U^n_m + N_0 W/N}, \tag{2}$$

where N_0, W, and U^n_m represent the noise power spectral density, the system bandwidth, and the interference power from the other macro BS, respectively. U^n_m is obtained by using the maximum transmit power of the macro BS and the channel gain from the other macro BS, which is located outside the macro cell. Moreover, $I^n_{b,m} = \sum_{j=1, j\neq b}^{B} h^n_{j,m} \sum_{r=1}^{M} s^n_{j,r} p^n_{j,r}$, where $p^n_{j,r}$ denotes the transmit power for user r on subchannel n at BS j, and $I^n_{b,m}$ represents the sum of inner macro-cell interference powers. It is noted that there is no NOMA-user interference in (2) since the SINRs are used only for SIC ordering. Let P^b_{max} denote the maximum transmit power of BS b. Then, $0 \le p^n_{b,m} \le P^b_{max}$, and $\sum_{n=1}^{N} \sum_{m=1}^{M} p^n_{b,m} = P^b_{max}$, where $p^n_{b,m}$ denotes the transmit power for user m on subchannel n at BS b. For SIC decoding, it is assumed that $\Gamma^n_{b,1} > \Gamma^n_{b,2} > \cdots > \Gamma^n_{b,M}$, without loss of generality.

Assuming perfect SIC, the received SINR of user m for BS b on subchannel n in downlink NOMA-based HetNet is obtained as

$$\gamma^n_{b,m} = \frac{s^n_{b,m} h^n_{b,m} p^n_{b,m}}{O^n_{b,m} + I^n_{b,m} + U^n_m + N_0 W/N}, \tag{3}$$

where $O^n_{b,m} = h^n_{b,m} \sum_{r=1}^{m-1} s^n_{b,r} p^n_{b,r}$, which corresponds to the aggregate NOMA-user interference powers. Using (3), the achievable data rate of user m for BS b on subchannel n is then expressed as

$$R^n_{b,m} = \frac{W}{N} \log_2(1 + \gamma^n_{b,m}). \tag{4}$$

Aiming at maximizing the sum rate while the quality of service (QoS) of each user meets the minimum data-rate requirement, denoted by R_{thr}, the optimization problem of user association, subchannel allocation, and power allocation in the downlink NOMA-based HetNet can be formulated by using (4) as follows:

$$\max \sum_{n=1}^{N} \sum_{b=1}^{B} \sum_{m=1}^{M} x_{b,m} R^n_{b,m}, \tag{5a}$$

$$\text{s.t.} \sum_{b=1}^{B} x_{b,m} = 1, \quad \forall m \in \mathcal{M}, \tag{5b}$$

$$\sum_{n=1}^{N} s^n_{b,m} \le 1, \forall m \in \mathcal{M}, \quad \forall b \in \mathcal{B}, \tag{5c}$$

$$\sum_{n=1}^{N} \sum_{m=1}^{M} p^n_{b,m} = P^b_{max}, \quad \forall b \in \mathcal{B}, \tag{5d}$$

$$\sum_{n=1}^{N} \sum_{b=1}^{B} R^n_{b,m} \ge R_{thr}, \quad \forall m \in \mathcal{M}, \tag{5e}$$

where the first constraint in (5b) corresponds to the user association, and (5c) is associated with the subchannel allocation. Further, (5d) is related to the power allocation, while the last constraint in (5e) represents the minimum data-rate requirement. In this paper, we assume that an outage event occurs, when at least one user in the HetNet does not satisfy the minimum data-rate requirement, R_{thr}.

III. PROPOSED ALGORITHMS FOR SUBCHANNEL AND POWER ALLOCATION

A. USER ASSOCIATION AND SUBCHANNEL ALLOCATION SCHEME FOR NOMA

In this section, we describe the user association and subchannel allocation schemes for solving the optimization problem in (5). Analogous to the user association scheme in [8], the Lagrangian dual decomposition method for user association is adopted to relax the complexity of the objective function and the binary nature of variables in the set of user association indicators, X. By the Lagrangian dual decomposition-based user association scheme, each user in the HetNet chooses BS b^* that maximizes the relaxed problem of (5), which is given as

$$b^* = \underset{b}{\text{argmax}}(\log(\bar{R}^n_{b,m}) - \mu_b(t) + \nu_m(t)\bar{R}^n_{b,m}), \quad (6)$$

where the Lagrangian multipliers at the t-th iteration are $\mu_b(t) = \mu_b(t-1) - \delta_1(t-1)(K_b(t-1) - \sum_{m=1}^{M} x_{b,m}(t-1))$, and $\nu_m(t) = \nu_m(t-1) - \delta_2(t-1)(\sum_{b=1}^{B} x_{b,m}(t-1)\bar{R}^n_{b,m} - R_{thr})$. Moreover, $\delta_1(t)$ and $\delta_2(t)$ are the step sizes of Lagrangian multipliers, and $K_b(t) = e^{[\mu_b(t-1)-1]}$, which denotes the optimum association number of BS b. In (6), $\bar{R}^n_{b,m}$ is obtained by using (4) with only the path loss effect (i.e., $h^n_{b,m} = d^{-\alpha}_{b,m}$), and it is assumed that all the subchannel allocation indicators are one, and the transmit powers for users at each BS are fixed and equal. It is noted that the aim of the relaxed problem in (6) is to achieve the maximum sum rate and the load balancing while guaranteeing the first and the last constraints in (5).

After the user association process, each user is allocated to a subchannel that can maximize the sum rate. In [8], the two-sided matching scheme is presented for the subchannel allocation in NOMA-based HetNet. However, the matching algorithm may limit the NOMA gain, because at most two users can be allocated to one subchannel for NOMA. Therefore, to enhance the NOMA gain, we propose the subchannel allocation scheme with an iterative algorithm, as shown in Algorithm 1. The proposed subchannel allocation scheme calculates the achievable data rate of user m for the associated BS on subchannel n, i.e., $C^n_{b^*_m,m}$, and finds the optimal indices of the user and subchannel, i.e., m^* and n^*, in order to maximize $C^n_{b^*_m,m}$. Then, subchannel n^* is allocated to user m^* of BS b^*, and m^* is eliminated in set $\tilde{\mathcal{M}}$. After that, $C^n_{b^*_m,m}$ is recalculated by the updated subchannel indicators, and this procedure is repeated until $\tilde{\mathcal{M}}$ becomes empty. As a result, through Algorithm 1, the best subchannel is selected for a user to achieve the maximum sum rate in each iteration, which is different from a greedy scheduling algorithm, where a user with the highest data rate is selected for a given subchannel. It is noted that the numerator of SINR in $C^n_{b^*_m,m}$ is slightly different from that in (3), because the associated BS and the desired subchannel are considered in $C^n_{b^*_m,m}$.

Algorithm 1 Subchannel Allocation for NOMA-Based HetNet

1 Initialize channel gains, $h^n_{b,m}, \forall n \in \mathcal{N}, \forall b \in \mathcal{B}, \forall m \in \mathcal{M}$.
2 Initialize X using Lagrangian dual decomposition-based user association.
3 Set $p^n_{b^*_m,m} = P^b_{max}/M, \forall n \in \mathcal{N}, \forall m \in \mathcal{M}$.
4 Set $s^n_{b^*_m,m} = 0, \forall n \in \mathcal{N}, \forall m \in \mathcal{M}$.
5 Set $\tilde{\mathcal{M}} = \{1, \cdots, M\}$.
6 Calculate $C^n_{b^*_m,m} = \log_2\left(1 + \frac{x_{b^*_m,m} h^n_{b^*_m,m} p^n_{b^*_m,m}}{O^n_{b^*_m,m} + I^n_{b^*_m,m} + U^n_m + N_0 W/N}\right)$, $\forall n \in \mathcal{N}, \forall m \in \mathcal{M}$.
7 **while** $\tilde{\mathcal{M}} = \emptyset$ **do**
8 Select $(m^*, n^*) = \underset{m \in \tilde{\mathcal{M}}, n \in \mathcal{N}}{\text{argmax}} C^n_{b^*_m,m}$.
9 Set $s^{n^*}_{b^*_{m^*},m^*} = 1$.
10 Update $\tilde{\mathcal{M}} = \tilde{\mathcal{M}} \backslash \{m^*\}$.
11 Update $C^n_{b^*_m,m}, \forall n \in \mathcal{N}, \forall m \in \mathcal{M}$.
12 **end**

B. DEEP LEARNING-BASED POWER ALLOCATION SCHEME FOR NOMA

The problem of power allocation in (5a) with the constraints in (5d) and (5e) is non-convex. Thus, in this section, we propose the deep learning-based power allocation algorithm as a solution of the problem, where the user association and subchannel indicators, X and S, obtained in Section III-A, are used. In Fig. 2, we describe the proposed power allocation scheme for NOMA, where the input of DNN is the normalized channel gains in decibel (dB). Specifically, the normalization process in DNN can improve the training performance, and thus we employ the Z-score normalization process, which is expressed as

$$\hat{h}^n_{b,m} = \frac{\log_{10} h^n_{b,m} - \mathbb{E}[\log_{10} h^n_{b,m}]}{\sqrt{\mathbb{E}[(\log_{10} h^n_{b,m} - \mathbb{E}[\log_{10} h^n_{b,m}])^2]}}. \quad (7)$$

After the normalization of the channel gains, the DNN process is performed, where the setup of the proposed DNN structure is shown in Table 1. The proposed DNN structure consists of 4 hidden layers, and the size of each hidden layer is 512, where we adopt batch normalization and rectified linear unit (ReLU) in each layer, a ReLU performs the operation of $\max(\cdot, 0)$. Let the output of DNN be denoted as matrix $\boldsymbol{Z}$ whose size is $N \times B \times M$, where the (b, m)-th element of $\boldsymbol{Z}$ is denoted as $Z^n_{b,m}$. Then, the scheduling filtering is carried

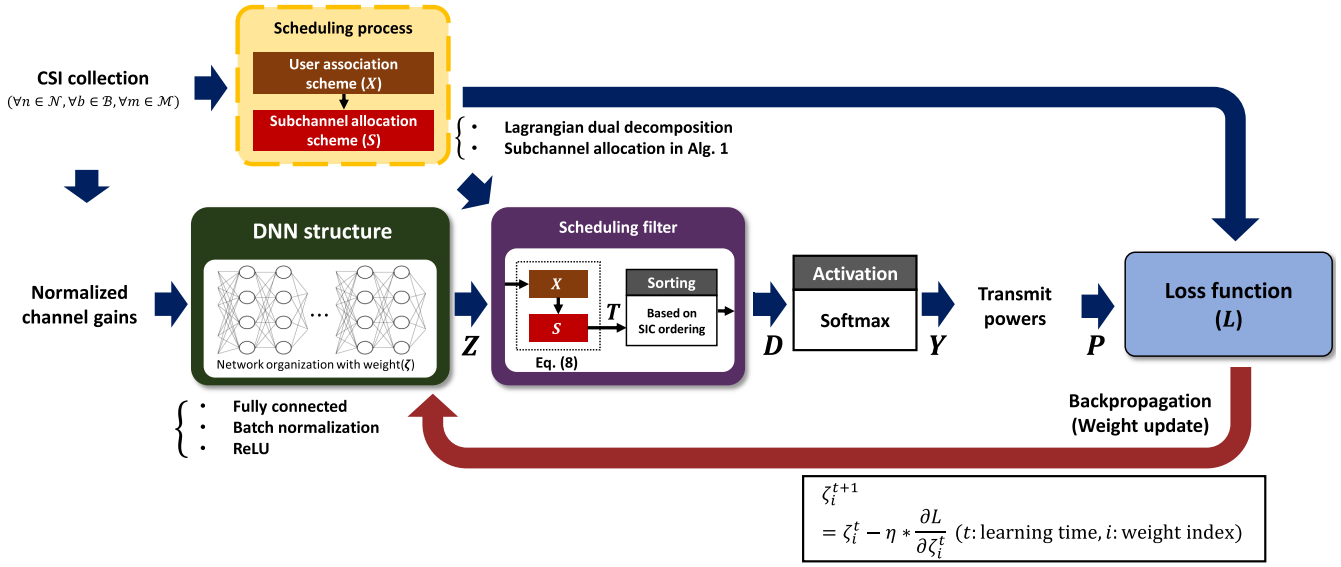

FIGURE 2. DNN-based transmit power allocation process for training.

TABLE 1. Description of DNN structure.

Name	Description
Layer	Fully connected layer
The number of hidden nodes	512
The number of hidden layers	4
Activation function	Rectified linear unit
Normalization	Batch normalization

out, where its inputs are the DNN output, $\boldsymbol{Z}$, and the user association and subchannel indicators, X and S. The output of the scheduling filter is matrix $\boldsymbol{T}$ whose size is $N \times B \times M$, and its (b, m)-th element, $T^n_{b,m}$, is obtained as

$$T^n_{b,m} = \begin{cases} -\infty & \text{if } x_{b,m} = 0 \text{ or } s^n_{b,m} = 0, \\ Z^n_{b,m} & \text{otherwise.} \end{cases} \tag{8}$$

Then, the elements of $\boldsymbol{T}$ are sorted in ascending order, where the arranged matrix is denoted as $\boldsymbol{D}$. The Softmax function is employed using the elements of $\boldsymbol{D}$, $D^n_{b,m}$, as follows:

$$Y^n_{b,m} = \frac{e^{D^n_{b,m}}}{\sum_{i=1}^{N}\sum_{j=1}^{M} e^{D^i_{b,j}}}. \tag{9}$$

The Softmax function in (9) can guarantee $\sum_{n=1}^{N}\sum_{m=1}^{M} Y^n_{b,m} = 1$, where the Softmax output, $Y^n_{b,m}$, is multiplied by P^b_{max}, and then the final transmit powers for NOMA, $p^n_{b,m}$, are obtained. In (9), it is considered that $0 \le p^n_{b,m} \le P^b_{max}$, and $\sum_{n=1}^{N}\sum_{m=1}^{M} p^n_{b,m} = P^b_{max}$.

In the training mechanism of our proposed deep-learning process, the transmit powers are optimized by minimizing the loss function. To solve the optimization problem in (5), the loss function is defined as

$$L = -\lambda \sum_{n=1}^{N}\sum_{b=1}^{B}\sum_{m=1}^{M} x_{b,m} R^n_{b,m} + \sum_{m=1}^{M} \frac{W}{N} \tanh\left(\left[R_{thr} - \sum_{n=1}^{N}\sum_{b=1}^{B} x_{b,m} R^n_{b,m}\right]^+\right), \tag{10}$$

where λ is the weight value that determines the priority level between maximizing the sum rate and achieving the minimum QoS requirement. In addition, tanh and $[\cdot]^+$ represent the hyperbolic tangent operation, and the ReLU function, respectively. It is noted that the loss function is defined to maximize the sum rate while achieving the minimum data-rate requirement. Furthermore, the weight values in the DNN structure are optimized by the loss function. Letting the weight matrix for all of the DNN structures be denoted as $\boldsymbol{\zeta}$, each of the weight values is updated by $\zeta_i^{t+1} = \zeta_i^t - \eta \frac{\partial L}{\partial \zeta_i^t}$, where t, i, and η are the learning time, the index of the weight matrix, $\boldsymbol{\zeta}$, and the learning rate, respectively. Through updating the weight values in the DNN structure, the power allocation coefficients are successfully converged.

The algorithm of the training process for NOMA power allocation is described in Algorithm 2, where the transmit powers are allocated to only the selected NOMA users by Algorithm 1.

IV. SIMULATION RESULTS

In this section, we show the simulation results of the proposed subchannel and power allocation scheme (Prop-SPA), which includes the Lagrangian dual decomposition-based user association, Algorithm 1-based subchannel allocation, and Algorithm 2-based power allocation schemes. For simulations, we assume the following parameters which are

Algorithm 2 DNN-Based Training Process for NOMA Power Allocation

Initialize channel gains, $h^n_{b,m}$, and normalized channel gains, $\hat{h}^n_{b,m}$, $\forall n \in \mathcal{N}$, $\forall b \in \mathcal{B}$, $\forall m \in \mathcal{M}$.
Initialize user association and subchannel indicators, X and S.
Initialize trainable values of DNN structure.
for *every training epoch* **do**
  for *every batch data* **do**
    The users are excluded in the training phase by scheduling filter in (8).
    For selected users, the transmit powers are allocated by (9) in multiple subchannels.
    Trainable values in the proposed DNN structure are optimized by the loss function, L, in (10).
  end
end

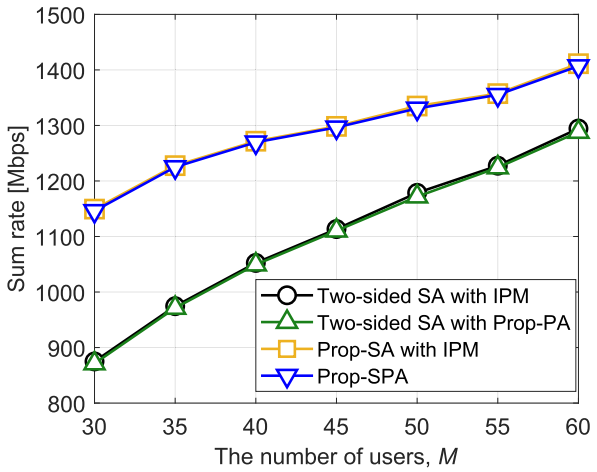

FIGURE 3. Sum rate of the two-sided matching, IPM, and proposed schemes for the number of users when $N = 20$ and $B = 4$.

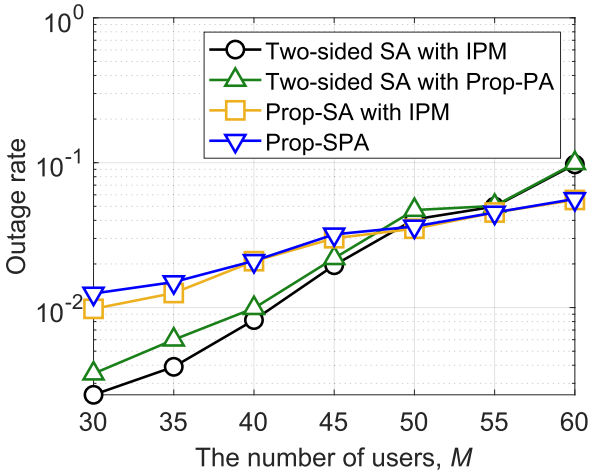

FIGURE 4. Outage rate of the two-sided matching, IPM, and proposed schemes for the number of users when $N = 20$ and $B = 4$.

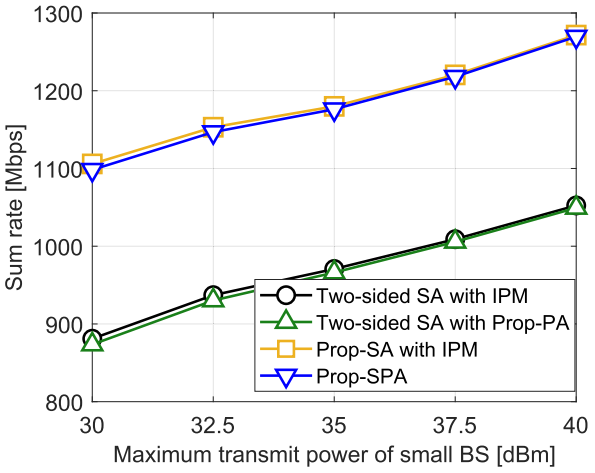

FIGURE 5. Sum rate of the two-sided matching, IPM, and proposed schemes for the maximum transmit power of the small BSs when $N = 20$, $B = 4$, and $M = 40$.

TABLE 2. Simulation parameters.

Parameters	Values
The number of BSs (B)	4
The number of users (M)	40
Maximum power of macro BS	43 dBm
Maximum power of small BSs	40 dBm
Noise spectral density (N_0)	-174 dBm/Hz
Bandwidth (W)	100MHz
Path loss exponent (α)	3.0
Data rate requirement (R_{thr})	1.0 Mbps

described in Table 2 [25], [26], [27], where the macro BS is located at the center of the macro cell with a radius of 500m (i.e., the origin in the two-dimensional plane), and the three small BSs are located at (250m, 0°), (250m, 120°), and (250m, 240°) in the two-dimensional polar coordinate system, respectively. Moreover, the other macro BS is located 1,000m away from the origin. In addition, training epochs, batch size, and learning rate are set to 100, 1,000, and 0.001, respectively. Furthermore, 20,000 and 10,000 channel realizations are randomly generated by using (1) for training and testing simulations, respectively. It is noted that the channel samples are independently generated in each phase, where the Rayleigh fading channel coefficients, $g^n_{b,m}$, $\forall n \in \mathcal{N}$, $\forall b \in \mathcal{B}$, $\forall m \in \mathcal{M}$, are the independent complex Gaussian random variables with zero mean and unit variance. In addition, the path loss components, $d_{b,m}$, $\forall b \in \mathcal{B}$, $\forall m \in \mathcal{M}$, are determined by the uniformly distributed users in a macro cell. The weight value of λ in (10) is set to 0.001, where the weight value is the optimal value that maximizes the sum rate while guaranteeing the minimum QoS requirement, which is found by exhaustive search, as in [19] and [28].

To better evaluate our proposed scheme, Prop-SPA, we compare its performance in terms of sum rate and outage rate with various combinations of baseline approaches such as the two-sided matching-based subchannel allocation scheme

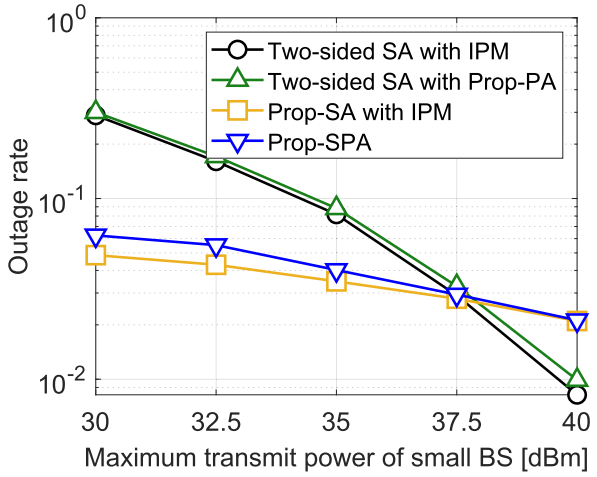

FIGURE 6. Outage rate of the two-sided matching, IPM, and proposed schemes for the maximum transmit power of the small BSs when $N = 20$, $B = 4$, and $M = 40$.

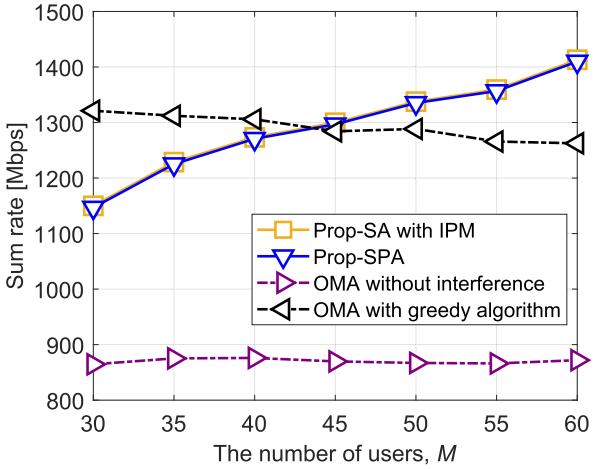

FIGURE 7. Sum rate of the OMA-based schemes and the proposed schemes for the number of users of the small BSs when $N = 20$, $B = 4$, and $M = 40$.

with IPM-based power allocation (Two-sided SA with IPM), the two-sided matching-based subchannel allocation scheme with Algorithm 2-based power allocation (Two-sided SA with Prop-PA), and the Algorithm 1-based subchannel allocation scheme with IPM-based power allocation (Prop-SA with IPM). The two-sided matching scheme which is illustrated in [8] can improve the sum-rate performance with the many-to-many matching-based algorithm. However, the matching algorithm has the disadvantage of focusing only on channel gain-based matching without considering the data rate. Therefore, two-sided matching-based subchannel allocation may not achieve the maximum sum rate. On the other hand, the IPM scheme, which is illustrated in [12], can be considered as an optimal power allocation scheme to resolve a non-convex problem such as (5), where it requires huge computational complexity due to finding a global optimum solution.

Figs. 3 and 4 show the results of the sum rate and outage rate, respectively, for various subchannel and power allocation schemes, when M varies from 30 to 60, while $N = 20$ and $B = 4$. In Fig. 3, the sum rates of all the subchannel and power allocation schemes increase, as M increases, since more multiplexing gain can be achieved through NOMA with a more number of users. Prop-SPA can provide almost the same sum rate as Prop-SA with IPM, while it requires significantly lower complexity for training compared to Prop-SA with IPM. In addition, the sum rate of Prop-SPA is considerably better than Two-sided SA with IPM and Prop-PA because the proposed Algorithm 1-based subchannel allocation can benefit from higher NOMA gain compared to the two-sided matching.

In Fig. 4, the outage rate results of all the schemes become worse, as M increases. The outage rates of Two-sided SA with IPM and Prop-PA are better compared to Prop-SPA for small M, whereas Prop-SPA provides better outage rates compared to Two-sided SA with IPM and Prop-PA for large M. The reason is that Prop-SPA has the lower powers of the desired signals for small M but higher NOMA gain for large M compared to Two-sided SA with IPM and Prop-PA. In addition, the outage rate of Prop-SPA is close to that of Prop-SA with IPM, as shown in Fig. 3.

Figs. 5 and 6 illustrate the sum rate and outage rate, respectively, for the four different subchannel and power allocation schemes, when $N = 20, M = 40, B = 4$, and P_{max}^{k} changes from 30 to 40 dBm for the small BSs (i.e., $k = 2, 3, 4$). In Fig. 5, the sum rates of all the schemes increase with a rise in the maximum power of the small BSs. Prop-SPA provides significantly better sum rates compared to Two-sided SA with IPM and Prop-PA for all cases, and it has a similar sum rate to Prop-SA with IPM. In Fig. 6, Prop-SPA has better outage performance compared to Two-sided SA with IPM and Prop-PA for low transmit powers of the small BSs, but it has worse performance than those for high transmit powers of the small BSs. Prop-SPA achieves slightly worse outage rates than Prop-SA with IPM. In Figs. 4 and 6, it is noted that the outage rate of Prop-SPA is less sensitive to both the number of users and the transmit power of the small BSs, while the outage rates of Two-sided SA are highly subject to them. Therefore, considering the given system parameters, we can selectively use the two depending on the outage and complexity requirements, while Prop-SPA always provides higher sum rates.

We further compare our proposed scheme with orthogonal multiple access (OMA)-based subchannel allocation schemes in terms of the sum rate and outage rate, where two OMA-based subchannel allocation schemes are considered to maximize the sum rate. The first OMA-based scheme does not allow interference between small cells and between a macro cell and a small cell in subchannel allocation, which can limit the spectral efficiency performance. In contrast, the second OMA-based scheme with greedy algorithm allows the co-tier interference (i.e., interference

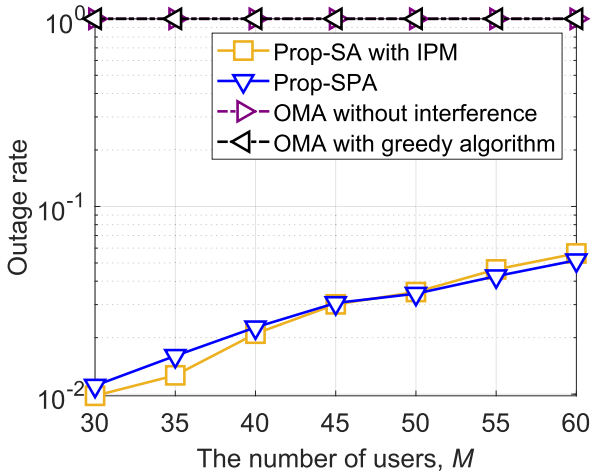

FIGURE 8. Outage rate of the OMA-based schemes and the proposed schemes for the number of users of the small BSs when $N = 20$, $B = 4$, and $M = 40$.

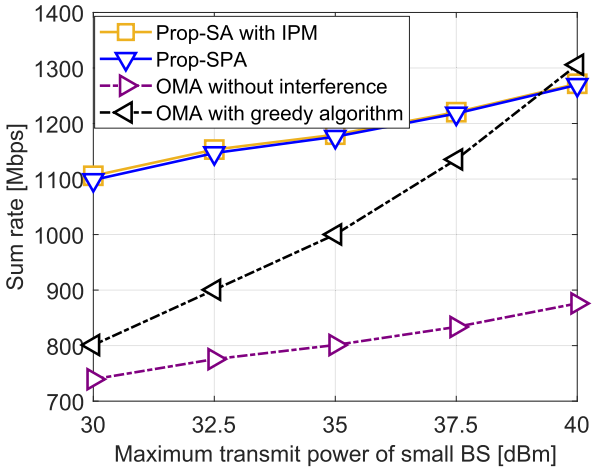

FIGURE 9. Sum rate of the OMA-based schemes and the proposed schemes for the maximum transmit power of the small BSs when $N = 20$, $B = 4$, and $M = 40$.

between small cells) in subchannel allocation to improve the spectral efficiency, as in [29] and [30]. It is noted that both OMA-based schemes consider the subchannels with equal bandwidth, which depends on the total number of users, i.e., W/M, and they allocate equal transmit powers to all the subchannels. Figs. 7-10 show the performance comparisons between the proposed scheme and the two OMA-based schemes, where the first and second OMA-based schemes are referred to as OMA without interference and OMA with greedy algorithm, respectively.

Figs. 7 and 8 show the results of the sum rate and outage rate for the proposed and OMA-based schemes with various M when $N = 20$ and $B = 4$, respectively. In Fig. 7, the OMA with greedy algorithm has superior sum-rate results compared to the OMA without interference because of the subchannel reuse. In addition, when compared to NOMA-based algorithms, the OMA with greedy algorithm provides higher sum-rate performance than the Prop-SA with IPM and Prop-SPA for small M. However, in Fig. 8, both OMA-based schemes show considerably worse outage performance than the proposed schemes due to the limitation of resource utilization of OMA and no consideration of the minimum data-rate requirement. Therefore, it is shown that the proposed NOMA-based resource allocation is more suitable to improve the sum-rate performance while guaranteeing the QoS requirement. Similarly, Figs. 9 and 10 show the results of the sum rate and outage rate for proposed and OMA-based schemes with different P_{max}^{k} of small BSs when $N = 20$, $M = 40$, and $B = 4$, respectively. Analogous to Figs. 7 and 8, Figs. 9 and 10 demonstrate that the Prop-SA with IPM and Prop-SPA achieve significantly better sum rate and outage rate compared to the OMA-based schemes. However, the OMA with greedy algorithm can provide better sum rate than the proposed NOMA-based schemes for high P_{max}^{k} of small BSs.

Fig. 11 shows the total computational times of all the schemes for training, which are obtained for 20,000 channel

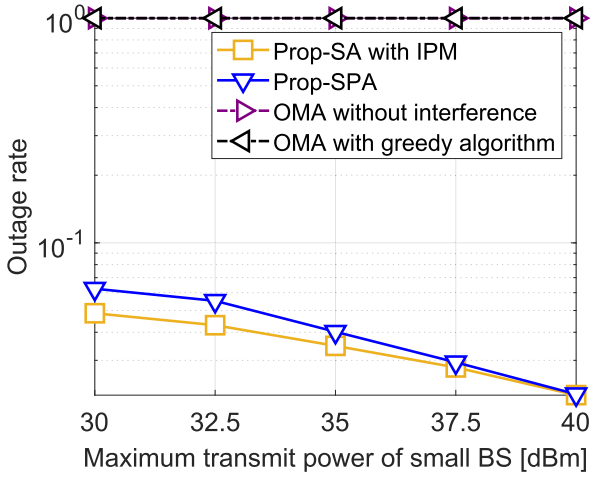

FIGURE 10. Outage rate of the OMA-based schemes and the proposed schemes for the maximum transmit power of the small BSs when $N = 20$, $B = 4$, and $M = 40$.

realizations. The results of the two schemes with IPM can be regarded as the computational time of DNN-based supervised learning for training. In the figure, the computational times of Prop-SPA and Two-sided SA with Prop-PA are considerably shorter than those of the schemes with IPM. Fig. 12 shows the computational times of Prop-SPA, Two-sided SA with Prop-PA, and OMA with greedy algorithm for testing, which are obtained for one channel realization. In the figure, Prop-SPA has more computational time than Two-sided SA with Prop-PA because the proposed subchannel allocation scheme requires more computational time than the two-sided matching-based subchannel allocation scheme. In addition, the OMA with greedy algorithm has the longest computational time compared to the DNN-based schemes. It is remarkably noted that the DNN-based algorithm can considerably reduce computational complexity compared to the conventional iterative algorithms. In Figs. 11 and 12, the

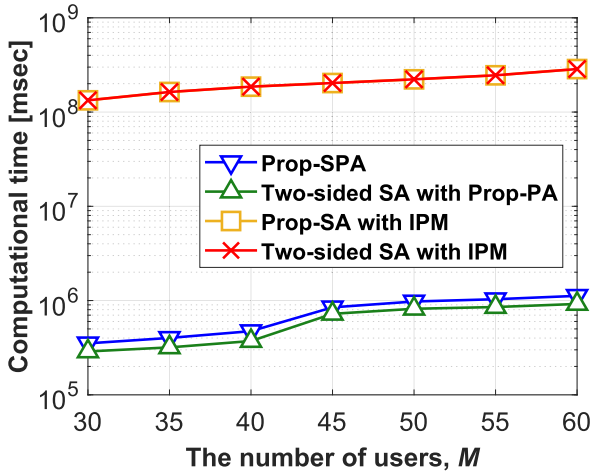

FIGURE 11. Computational times for training when $N = 20$ and $B = 4$.

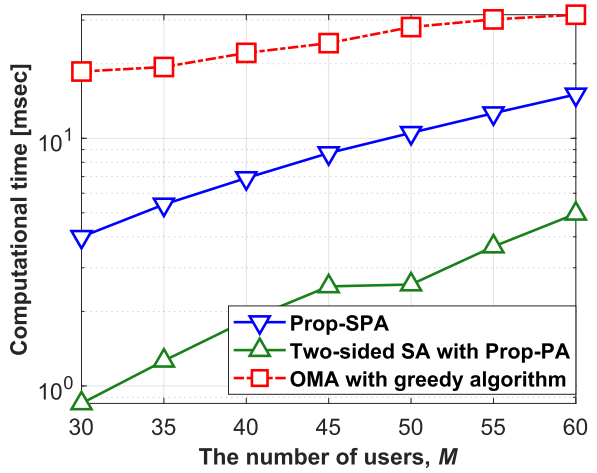

FIGURE 12. Computational times for testing when $N = 20$ and $B = 4$.

computational times of all the schemes increase with the number of users.

V. CONCLUSION

In this paper, we propose the iterative subchannel allocation scheme and the DNN-based power allocation scheme with unsupervised learning for downlink NOMA-based HetNet, where the optimization problem is formulated to maximize the sum rate with the minimum QoS requirement. The proposed power allocation scheme provides similar sum rate and outage performances to the IPM, which can give the optimal solution but with prohibitively higher complexity, compared to our proposed scheme. In addition, the proposed subchannel allocation scheme achieves more NOMA gain compared to the conventional two-sided matching scheme. In conclusion, our proposed resource allocation scheme is considerably superior to the conventional schemes in terms of the sum rate with the comparable outage rate.

REFERENCES

[1] V. W. Wong, R. Schober, D. W. K. Ng, and L.-C. Wang, *Key Technologies for 5G Wireless Systems*. Cambridge, U.K.: Cambridge Univ. Press, 2017.

[2] C.-H. Liu and D.-C. Liang, "Heterogeneous networks with power-domain NOMA: Coverage, throughput, and power allocation analysis," *IEEE Trans. Wireless Commun.*, vol. 17, no. 5, pp. 3524–3539, May 2018.

[3] Z. Zhang, G. Yang, Z. Ma, M. Xiao, Z. Ding, and P. Fan, "Heterogeneous ultradense networks with NOMA: System architecture, coordination framework, and performance evaluation," *IEEE Veh. Technol. Mag.*, vol. 13, no. 2, pp. 110–120, Jun. 2018.

[4] Q. Li, T. Shang, T. Tang, and Z. Xiong, "Adaptive user association scheme for indoor multi-user NOMA-VLC systems," *IEEE Wireless Commun. Lett.*, vol. 12, no. 5, pp. 873–877, May 2023.

[5] H. Xiao, W. Zhang, and A. T. Chronopoulos, "Joint subchannel and power allocation for energy efficiency optimization in NOMA heterogeneous networks with energy harvesting," *IEEE Syst. J.*, vol. 16, no. 3, pp. 4904–4915, Sep. 2022.

[6] S. Mirbolouk, M. Valizadeh, M. C. Amirani, and S. Ali, "Relay selection and power allocation for energy efficiency maximization in hybrid satellite-UAV networks with CoMP-NOMA transmission," *IEEE Trans. Veh. Technol.*, vol. 71, no. 5, pp. 5087–5100, May 2022.

[7] H. Zhang, S. Huang, C. Jiang, K. Long, V. C. M. Leung, and H. V. Poor, "Energy efficient user association and power allocation in millimeter-wave-based ultra dense networks with energy harvesting base stations," *IEEE J. Sel. Areas Commun.*, vol. 35, no. 9, pp. 1936–1947, Sep. 2017.

[8] H. Zhang, H. Zhang, K. Long, and G. K. Karagiannidis, "Deep learning based radio resource management in NOMA networks: User association, subchannel and power allocation," *IEEE Trans. Netw. Sci. Eng.*, vol. 7, no. 4, pp. 2406–2415, Oct. 2020.

[9] N. Yang, H. Zhang, K. Long, H.-Y. Hsieh, and J. Liu, "Deep neural network for resource management in NOMA networks," *IEEE Trans. Veh. Technol.*, vol. 69, no. 1, pp. 876–886, Jan. 2020.

[10] Q. Shi, M. Razaviyayn, Z.-Q. Luo, and C. He, "An iteratively weighted MMSE approach to distributed sum-utility maximization for a MIMO interfering broadcast channel," *IEEE Trans. Signal Process.*, vol. 59, no. 9, pp. 4331–4340, Sep. 2011.

[11] K. Shen and W. Yu, "Fractional programming for communication systems—Part I: Power control and beamforming," *IEEE Trans. Signal Process.*, vol. 66, no. 10, pp. 2616–2630, May 2018.

[12] U. F. Siddiqi, S. M. Sait, and M. Uysal, "Deep reinforcement based power allocation for the max-min optimization in non-orthogonal multiple access," *IEEE Access*, vol. 8, pp. 211235–211247, 2020.

[13] Y. Fu, W. Wen, Z. Zhao, T. Q. S. Quek, S. Jin, and F.-C. Zheng, "Dynamic power control for NOMA transmissions in wireless caching networks," *IEEE Wireless Commun. Lett.*, vol. 8, no. 5, pp. 1485–1488, Oct. 2019.

[14] J. Luo, J. Tang, D. K. C. So, G. Chen, K. Cumanan, and J. A. Chambers, "A deep learning-based approach to power minimization in multi-carrier NOMA with SWIPT," *IEEE Access*, vol. 7, pp. 17450–17460, 2019.

[15] W. Saetan and S. Thipchaksurat, "Power allocation for sum rate maximization in 5G NOMA system with imperfect SIC: A deep learning approach," in *Proc. 4th Int. Conf. Inf. Technol. (InCIT)*, Oct. 2019, pp. 195–198.

[16] Y. S. Nasir and D. Guo, "Multi-agent deep reinforcement learning for dynamic power allocation in wireless networks," *IEEE J. Sel. Areas Commun.*, vol. 37, no. 10, pp. 2239–2250, Oct. 2019.

[17] K. N. Doan, M. Vaezi, W. Shin, H. V. Poor, H. Shin, and T. Q. S. Quek, "Power allocation in cache-aided NOMA systems: Optimization and deep reinforcement learning approaches," *IEEE Trans. Commun.*, vol. 68, no. 1, pp. 630–644, Jan. 2020.

[18] W. Lee, M. Kim, and D.-H. Cho, "Transmit power control using deep neural network for underlay device-to-device communication," *IEEE Wireless Commun. Lett.*, vol. 8, no. 1, pp. 141–144, Feb. 2019.

[19] D. Kim, H. Jung, and I.-H. Lee, "Deep learning-based power control scheme with partial channel information in overlay device-to-device communication systems," *IEEE Access*, vol. 9, pp. 122125–122137, 2021.

[20] W. Lee and K. Lee, "Deep learning-based transmit power control for wireless-powered secure communications with heterogeneous channel uncertainty," *IEEE Trans. Veh. Technol.*, vol. 71, no. 10, pp. 11150–11159, Oct. 2022.

[21] W. Lee, M. Kim, and D.-H. Cho, "Deep learning based transmit power control in underlaid device-to-device communication," *IEEE Syst. J.*, vol. 13, no. 3, pp. 2551–2554, Sep. 2019.

[22] L. Dai, B. Wang, Z. Ding, Z. Wang, S. Chen, and L. Hanzo, "A survey of non-orthogonal multiple access for 5G," *IEEE Commun. Surveys Tuts.*, vol. 20, no. 3, pp. 2294–2323, 3rd Quart., 2018.
[23] A. N. Mohammed, M. E. Eltayeb, and I. Kostanic, "Channel estimation in millimeter wave systems with inter cell interference," in *Proc. IEEE 90th Veh. Technol. Conf. (VTC-Fall)*, Sep. 2019, pp. 1–5.
[24] S. Rezvani, E. A. Jorswieck, N. M. Yamchi, and M. R. Javan, "Optimal SIC ordering and power allocation in downlink multi-cell NOMA systems," *IEEE Trans. Wireless Commun.*, vol. 21, no. 6, pp. 3553–3569, Jun. 2022.
[25] J. Zhao, Y. Liu, K. K. Chai, A. Nallanathan, Y. Chen, and Z. Han, "Spectrum allocation and power control for non-orthogonal multiple access in HetNets," *IEEE Trans. Wireless Commun.*, vol. 16, no. 9, pp. 5825–5837, Sep. 2017.
[26] C. Chaieb, F. Abdelkefi, and W. Ajib, "Deep reinforcement learning for resource allocation in multi-band and hybrid OMA-NOMA wireless networks," *IEEE Trans. Commun.*, vol. 71, no. 1, pp. 187–198, Jan. 2023.
[27] H. Z. Khan, M. Ali, I. Rashid, A. Ghafoor, and M. Naeem, "Cell association for energy efficient resource allocation in decoupled 5G heterogeneous networks," in *Proc. IEEE 91st Veh. Technol. Conf. (VTC-Spring)*, May 2020, pp. 1–5.
[28] D. Kim, H. Jung, and I.-H. Lee, "User selection and power allocation scheme with SINR-based deep learning for downlink NOMA," *IEEE Trans. Veh. Technol.*, vol. 72, no. 7, pp. 8972–8986, Jul. 2023.
[29] K. Aghababaiyan and B. Maham, "QoS-aware downlink radio resource management in OFDMA-based small cells networks," *IET Commun.*, vol. 12, no. 4, pp. 441–448, Feb. 2018.
[30] K. Aghababaiyan and B. Maham, "Downlink radio resource allocation in OFDMA-based small cells networks," in *Proc. IEEE Int. Black Sea Conf. Commun. Netw. (BlackSeaCom)*, Jun. 2017, pp. 1–5.

DONGHYEON KIM (Graduate Student Member, IEEE) received the B.S. and M.S. degrees from Hankyong National University, South Korea, in 2020 and 2022, respectively. He is currently pursuing the Ph.D. degree in electronics and information convergence engineering with Kyung Hee University, South Korea. His current research interests include wireless communications, resource allocation, and deep learning algorithms.

SEAN (SEOK-CHUL) KWON (Member, IEEE) received the B.Sc. degree from Yonsei University, Seoul, South Korea, in 2001, the M.Sc. degree from the University of Southern California, Los Angeles, USA, in 2007, and the Ph.D. degree from the Georgia Institute of Technology, Atlanta, USA, in December 2013. He performed research with the Intel's Next Generation and Standards Division, Communication and Devices Group, from 2015 to 2017, where he contributed to 5G MIMO standards, the associated system design and patents. He has been an Assistant Professor with California State University Long Beach, and the Chief Director/Founder of the Wireless Systems Evolution Laboratory (WiSE Lab), since 2017. He also conducted postdoctoral research with the Wireless Devices and Systems Group, University of Southern California, from 2014 to 2015. He worked on CDMA common air interface focusing on layer-3 protocols with the Research and Development Institute, Pantech Company Ltd., Seoul, in 2001 to 2004. He was involved in several projects, such as a DARPA Project, an U.S. Army Research Laboratory Project, and six mobile-station projects for Motorola and Sprint, which were successfully on the market. His current research interests include 5G and beyond-5G wireless systems/network design, satellite communications, polarization diversity, and multiplexing, body area networks, such as wearable computing, wireless channel modeling and its applications, and the application of machine learning for wireless communications and signal processing. He was a recipient of three best paper awards from IEEE Green Energy and Smart Systems Conference (IGESSC), in 2018, 2019, and 2020.

HAEJOON JUNG (Senior Member, IEEE) received the B.S. degree (Hons.) in electrical engineering from Yonsei University, South Korea, in 2008, and the M.S. and Ph.D. degrees in electrical engineering from the Georgia Institute of Technology (Georgia Tech), Atlanta, GA, USA, in 2010 and 2014, respectively. From 2014 to 2016, he was a Wireless Systems Engineer with Apple, Cupertino, CA, USA. From 2016 to 2021, he was with Incheon National University, Incheon, South Korea. Since September 2021, he has been with the Department of Electronic Engineering, Kyung Hee University, as an Associate Professor. His research interests include communication theory, wireless communications, wireless power transfer, and statistical signal processing. He was a recipient of the Haedong Young Scholar Award from the Korean Institute of Communications and Information Sciences (KICS), in 2022. He is serving as an Editor for IEEE COMMUNICATIONS LETTERS and *ICT Express*.

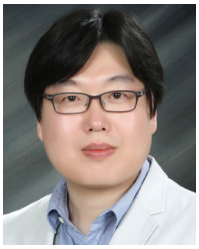

IN-HO LEE (Senior Member, IEEE) received the B.S., M.S., and Ph.D. degrees in electrical engineering from Hanyang University, Ansan, South Korea, in 2003, 2005, and 2008, respectively. He worked for LTE-Advanced standardization with Samsung Electronics Company, from 2008 to 2010. He was a Postdoctoral Fellow with the Department of Electrical Engineering, Hanyang University, from April 2010 to March 2011. Since March 2011, he has been a Professor with the School of Electronic and Electrical Engineering, Hankyong National University, Anseong-si, South Korea. From February 2017 to February 2018, he was a Visiting Associate Professor with the Department of Electrical and Computer Engineering, The University of British Columbia, Vancouver, Canada. His current research interests include non-orthogonal multiple access, millimeter wave wireless communications, cooperative communications, multi-hop relaying, the transmission and reception of multiple-input and multiple-output communications, multicast communications, and deep-learning algorithms.